

ELASTIC WAVE PROPAGATION IN AN INFINITE MEDIA

Zhongqing You and William Lord

Department of Electrical Engineering and Computer Engineering
Iowa State University
Ames, Iowa 50011

INTRODUCTION

For most of the complicated geometries encountered in ultrasonic nondestructive evaluation (NDE) applications, finite element (FE) solutions [1-4] of the elastic wave equation are usually limited because of the spatial discretization required for accuracy. Artificial boundaries introduced to limit the spatial dimensions of a given problem can cause unwanted reflections which corrupt the desired response. The simplest approach to this problem is to ensure that the model is large enough for the unwanted reflections to be separated from the desired signal in the time domain. But this becomes very expensive for most applications, especially for full 3-D geometries. Models for infinite media, therefore, are very important for numerical modeling in 3-D and even in many 2-D practical applications.

Waves in infinite media can be modeled by special elements or special boundary conditions referred to as infinite elements and energy-absorbing boundaries. Infinite elements or consistent boundaries [5,6] are not applicable to time domain FE solutions because they can only be used in the frequency domain, even though they constitute perfect absorbers for all wave types. Clayton and Engquist [7] derive a family of boundary conditions for numerical wave simulations based on paraxial approximations of the scalar and elastic wave equation. These boundary conditions can be implemented with varying degrees of accuracy. The equations, however, are more suited to finite difference formulations and are not readily implemented in the FE approach.

For time domain FE simulations of ultrasonic NDT phenomena in infinite media, it is easiest to use viscous boundary conditions [8]. In essence, these conditions can be interpreted as dashpots connected to the boundary points whose constants are a function of the material properties at that location. A review and application of this technique is given in the next section.

All of the local boundaries, which are characterized by their spatial and temporal natures, are based on physical (e.g. viscous boundary) or mathematical (e.g. paraxial) approximations. In many NDT applications the wanted signals are so weak that they are about the same order of magnitude as the small reflections from the artificial boundaries. A perfect absorber or non-reflecting boundary, therefore, is particularly desirable. Smith [9] proposes an approach to eliminate the reflection without approximations. With this approach, the simulations are done at least twice with different boundary conditions, and the results are summed to cancel the reflections as described in Section 3.

A detailed review and comparison of different techniques for numerical simulation of wave propagation problems in infinite media can be found in reference [10]. This paper is primarily concerned with the application of these techniques to ultrasonic NDT phenomena.

VISCOUS BOUNDARY

The viscous boundary conditions are:

$$\sigma = a \rho V_L \dot{u}_n \quad (1)$$

$$\tau = b \rho V_s \dot{u}_t \quad (2)$$

where

σ, τ = normal and tangential component of the surface traction;

ρ = material density;

V_L, V_s = longitudinal and shear velocities;

\dot{u}_n, \dot{u}_t = normal and tangential component of the velocity on the surface; and

a, b = constants.

For isotropic media, the displacement can be described by two potentials, ϕ and ψ , through Helmholtz decomposition. In the case of 2-D geometries with plane strain constraints, ψ is simplified to be a scalar:

$$u_x = \frac{\partial \phi}{\partial x} - \frac{\partial \psi}{\partial z} \quad (3)$$

$$u_z = \frac{\partial \phi}{\partial z} + \frac{\partial \psi}{\partial x} \quad (4)$$

Assume a plane incident L-wave with incident angle θ as shown in Fig. 1:

$$\phi = \rho^{ik_L(V_L t + z \cos \theta - x \sin \theta)} + A \rho^{ik_L(V_L t - z \cos \theta - x \sin \theta)} \quad (5)$$

$$\psi = B \rho^{iks(V_s t - z \cos \nu - x \sin \nu)} \quad (6)$$

where

$$k_L = \frac{\omega}{V_L} \quad , \quad k_s = \frac{\omega}{V_s}$$

A and B are the amplitude of the reflected L- and S-waves, respectively, and the elasticity gives

$$\sigma = \sigma_{zz} = \rho \left(V_L^2 - 2V_s^2 \right) \frac{\partial u_x}{\partial x} + \rho V_L^2 \frac{\partial u_z}{\partial z} \quad (7)$$

$$\tau = \sigma_{zx} = \frac{1}{2} \rho V_s^2 \left(\frac{\partial u_z}{\partial x} + \frac{\partial u_x}{\partial z} \right) \quad (8)$$

substituting Eqs. (3) through (8) into Eqs. (1) and (2) yields

$$(1 - 2S^2 \sin^2 \theta + a \cos \theta) A + (\sin 2\nu + a \sin \theta) B = 2S^2 \sin^2 \theta - 1 + a \cos \theta \quad (9)$$

$$(b \sin \nu + S^2 \sin 2\theta) A - (\cos 2\nu + b \cos \theta) B = S^2 \sin 2\theta - b \sin \nu \quad (10)$$

where

$$S = \frac{V_s}{V_L}$$

$$\frac{\sin \theta}{V_L} = \frac{\sin \nu}{V_s}$$

Assuming $A = B = 0$ yields

$$a = \frac{1 - 2S^2 \sin^2 \theta}{\cos \theta} \quad (11)$$

$$b = \frac{S^2 \sin 2\theta}{\sin \nu} \quad (12)$$

These are the conditions for the perfect absorber.

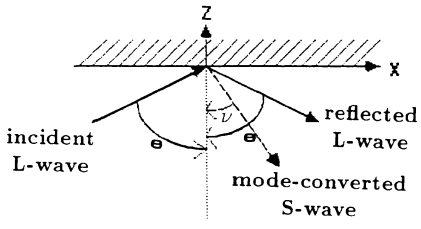


Fig. 1. Incident L-wave at a boundary.

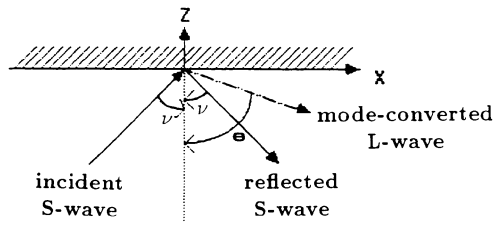


Fig. 2. Incident S-wave at a boundary.

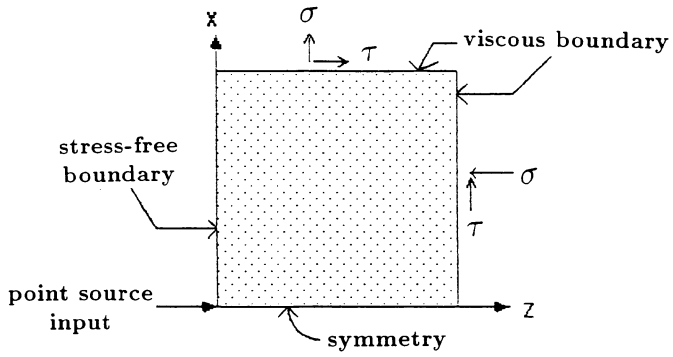


Fig. 3. Geometry of a half-space problem excited by a line source.

For incident S-wave with incident angle ν , similar derivation yields the condition for the perfect absorber:

$$a = \frac{\sin 2\nu}{\sin \theta} \quad (13)$$

$$b = \frac{\cos 2\nu}{\cos \nu} \quad (14)$$

where ν is the incident angle as shown in Fig. 2.

It should be noted that a and b are all independent of frequency, which implies that they can be used in the time domain.

For surface waves, Lysmer and Kuhlemeyer [8] derive an expression for a and b which is dependent on the frequency. This means that no perfect absorber can be obtained for a surface wave.

The implementation of the perfect absorbing boundary requires a priori information of the incident angle, which is not available in most cases. The standard absorbing boundary defined by $a = b = 1$, therefore, is recommended by Lysmer and Kuhlemeyer [8]. From Eqs. (11) through (14), the standard viscous boundary is a perfect absorber only when $V_S = \frac{1}{2}V_L$ and the incident wave is normal to the surface. The results in Fig. 4 are from the geometry shown in Fig. 3. It can be seen that the L-wave reflection is smaller than the S-wave reflection, even though they are all very weak. As for the Rayleigh wave, however, the standard absorbing boundary reflects about 15% of the displacement amplitude.

White, et al. [11] presents a unified boundary condition on the basis of a systematic formulation that is also applicable to anisotropic materials. For isotropic media, the first approximation of the constants a and b can be evaluated as

$$a = \frac{8}{15\pi}(5 + 2S - 2S^2) \quad (15)$$

$$b = \frac{8}{15\pi}(3 + 2S) \quad (16)$$

which are independent of both frequency and incident angle. The final values of a and b are optimized by maximizing the efficiency of the viscous boundary, which is defined as a weighted mean ratio of the absorbed energy to the energy arriving on the boundary. Using the a and b values, the example in Fig. 3 is recalculated with the results shown in Fig. 5. It can be seen that the reflections (especially the Raleigh wave reflection) are much smaller than for the standard viscous boundary.

Viscous boundaries are easy to implement and are not costly in terms of CPU-time and memory. They are not, however, very effective in absorbing Raleigh and shear waves. If a time-gate can distinguish the reflected shear and Raleigh waves from the wanted signal, this method could be very useful.

NON-REFLECTING BOUNDARY

Reflections can be completely eliminated by the superposition of solutions from the different boundary conditions [9]. This section is devoted to both analytical and numerical verification of this phenomenon and the application to NDT geometries.

Following the notations in the previous section, consider the incident L-wave as shown in Fig. 1. Imposing the boundary condition

$$u_z = 0, \quad \frac{\partial u_x}{\partial z} = 0 \quad \text{at } z = 0$$

results in $A = 1, B = 0$, while the boundary condition

$$u_x = 0, \quad \frac{\partial u_z}{\partial z} = 0 \quad \text{at } z = 0$$

gives $A = -1, B = 0$. Addition of these two solutions exactly cancels the reflection.

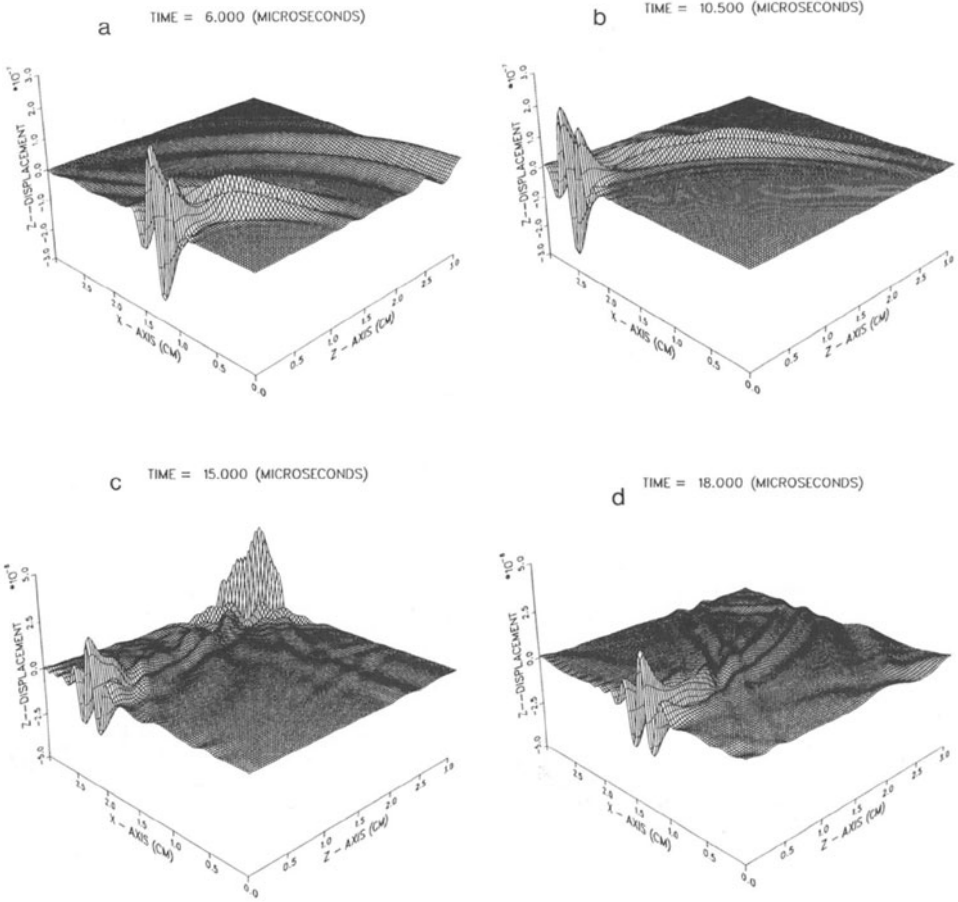


Fig. 4. Displacement plots of the wave interaction with a standard viscous boundary.

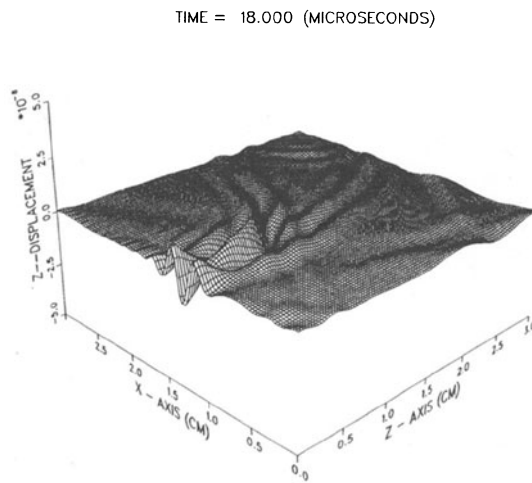


Fig. 5. Wave interactions with a unified viscous boundary.

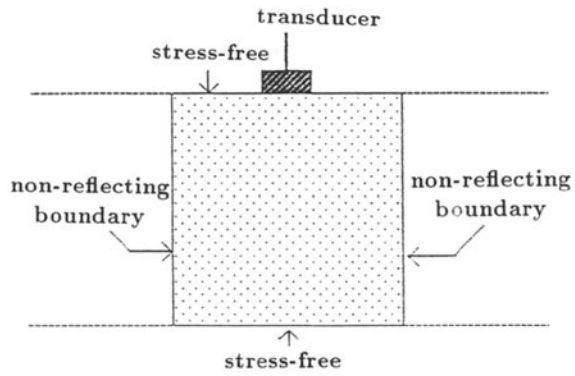


Fig. 6. Large plate inspection by a strip-like transducer.

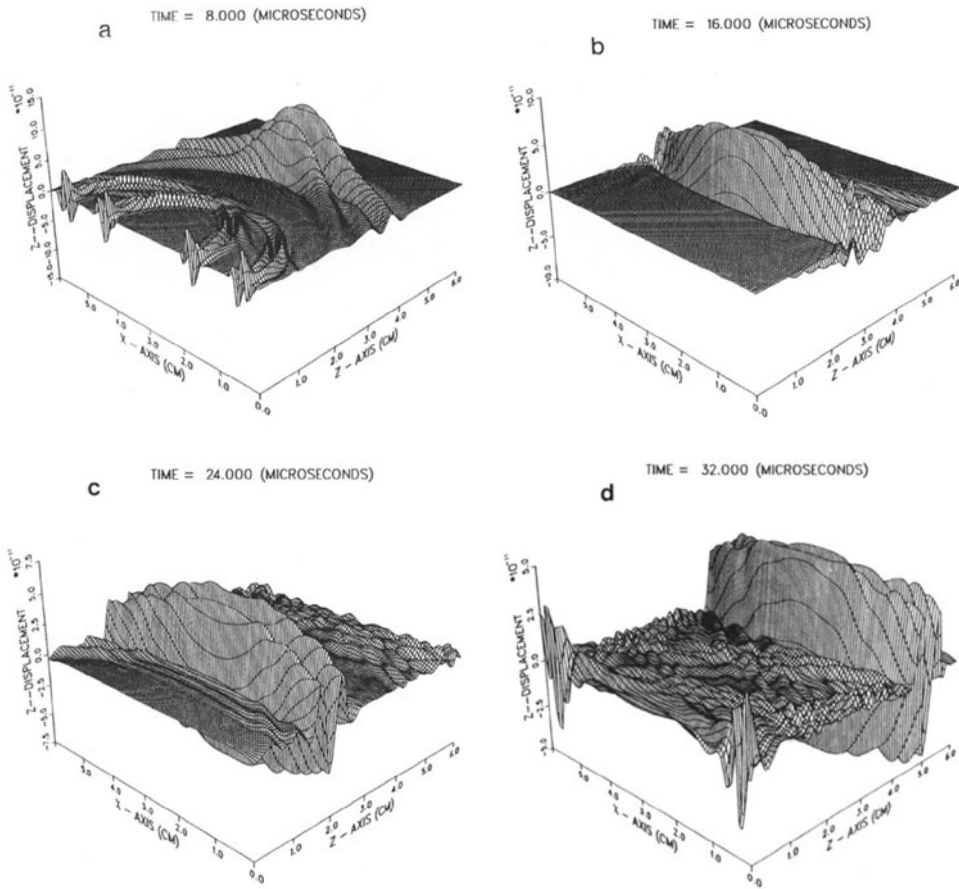


Fig. 7. Superposition of two solutions for the plate inspection problem as shown in Fig. 6.

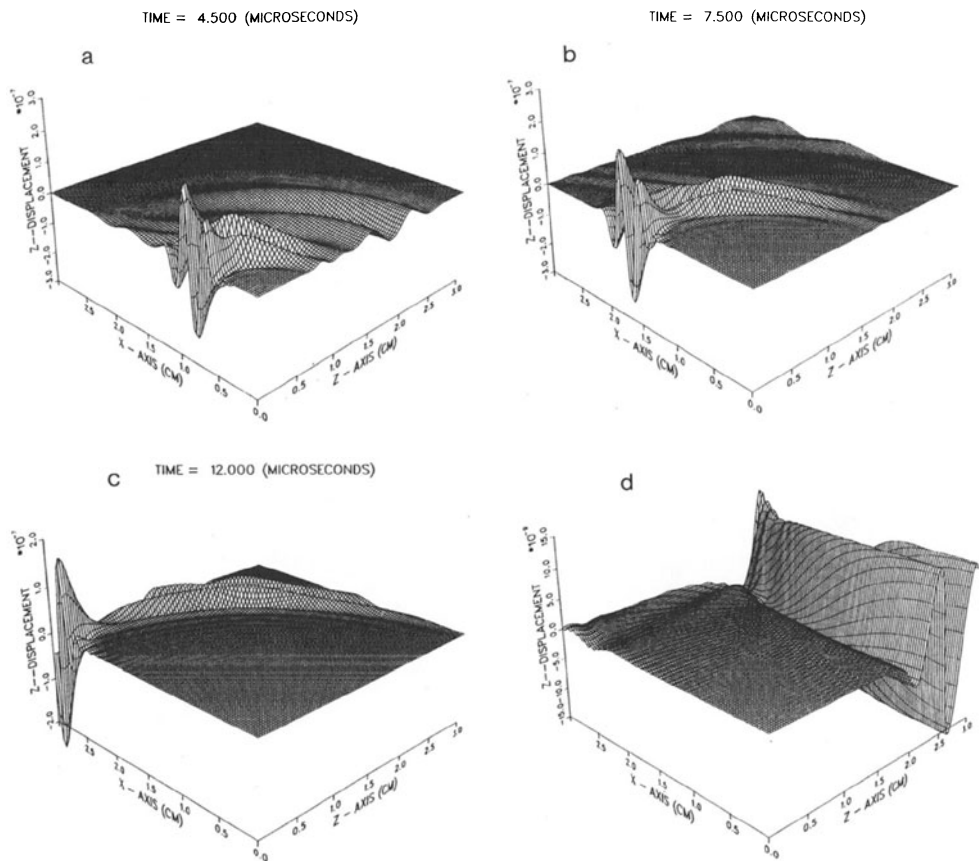


Fig. 8. Superposition of four solutions for the half-space problem as shown in Fig. 3.

The reflection cancellation is also true for shear and Rayleigh waves [9]. This is particularly useful because the viscous boundary cannot handle these types of waves efficiently.

For multiple reflection boundaries, the number of solutions needed to cancel all reflections is 2^n , where n = the number of multiple reflection boundaries. For the 2-D corner, $n = 2$, while $n = 3$ for the 3-D corner if all of the planes in the corner are artificial boundaries.

This model is applied to a common NDE example as shown in Fig. 6. Two boundary value problems are solved with different boundary conditions as

$$\text{Boundary Value Problem 1: } u_x^1 = 0, \frac{\partial u_z^1}{\partial x} = 0, u_x^2 = 0, \frac{\partial u_z^2}{\partial x} = 0$$

$$\text{Boundary Value Problem 2: } u_z^1 = 0, \frac{\partial u_x^1}{\partial x} = 0, u_z^2 = 0, \frac{\partial u_x^2}{\partial x} = 0$$

where the superscripts 1 and 2 represent the artificial boundary number. Addition of these two solutions is shown in Fig. 7 where the reflections from the artificial boundaries are completely eliminated in a time interval. The high order reflections show up delayed in time depending on the geometry. One non-reflecting boundary actually doubles the space in the direction of the surface normal.

For the geometry in Fig. 3, four solutions are required to cancel the reflections. Fig. 8 shows the results after the addition of those four solutions. It should be noted that the complete elimination of all waves is obtained in certain time periods.

CONCLUSION

For the purpose of NDE application, only two approaches are suitable for the finite element simulation of ultrasonic waves in infinite media. Viscous boundaries are recommended because of the easy implementation and cheap operation, even though it is only an approximation. Non-reflecting boundaries, on the other hand, are used only for those limited cases where a perfect absorber is necessary to obtain the desired signals.

REFERENCES

1. R. Ludwig and W. Lord, "A Finite Element Formulation for the Study of Ultrasonic NDT Systems," IEEE Transactions on Ultrasonics, Ferroelectrics and Frequency Control, Vol. 35, No. 6, pp. 809-820 (Nov., 1988).
2. R. Ludwig and W. Lord, "Developments in Finite Element Modeling of Ultrasonic NDT Phenomena," in Review of Progress in Quantitative NDE, edited by D. O. Thompson and D. E. Chimenti (Plenum Press, New York, 1986), Vol. 5A, pp. 73-81.
3. Z. You, W. Lord and R. Ludwig, "Numerical Modeling of Elastic Wave Propagation in Anisotropic Materials," in Review of Progress in Quantitative NDE, edited by D. O. Thompson and D. E. Chimenti (Plenum Press, New York, 1988), Vol. 7A, pp. 23-30.
4. Z. You and W. Lord, "Finite Element Study of Elastic Wave Interaction with Cracks," in Review of Progress in Quantitative NDE, edited by D. O. Thompson and D. E. Chimenti (Plenum Press, New York, 1989), Vol. 8A, pp. 109-116.
5. J. Lysmer and G. Waas, "Shear Waves in Plane Infinite Structures," Journal of the Engineering Mechanics Division, ASCE 98, pp. 85-105 (1972).
6. F. Kausel, J. M. Roedotdot sset, and G. Wars, "Dynamic Analysis of Footings on Layered Strata," Journal of the Engineering Mechanics Division, ASCE 103, pp. 569-588 (1975).
7. R. Clayton and B. Engquist, "Absorbing Boundary Conditions for Acoustic and Elastic Wave Equations," Bulletin of the Seismological Society of America, Vol. 67, No. 6, pp. 1529-1560 (1977).
8. J. Lysmer and R. L. Kuhlemeyer, "Finite Dynamic Model for Infinite Media," Journal of the Engineering Mechanics Division, ASC 95, pp. 859-877 (1969).
9. W. D. Smith, "A Nonreflecting Plane Boundary for Wave Propagation Problems," Journal of Computational Physics, Vol. 15, pp. 492-503 (1973).
10. E. Kausel and J. L. Tassoulas, "Transmitting Boundaries: A Closed-Form Comparison," Bulletin of the Seismological Society of America, Vol. 71, No. 1, pp. 143-159 (1981).
11. W. White, S. Valliappan and I. K. Lee, "Unified Boundary for Finite Dynamic Models," Journal of the Engineering Mechanics Division, ASCE 103, pp. 949-964 (1977).